How to cite: *Angew. Chem. Int. Ed.* **2023**, *62*, e202306315
doi.org/10.1002/anie.202306315

Bond Cleavage

Cleavage of Carbon Dioxide C=O Bond Promoted by Nickel-Boron Cooperativity in a PBP-Ni Complex

Lucía Álvarez-Rodríguez, Pablo Ríos, Carlos J. Laglera-Gándara, Andrea Jurado, Francisco José Fernández-de-Córdova, T. Brent Gunnoe, and Amor Rodríguez**

Abstract: The synthesis and characterization of (^{tBu}PBP)Ni(OAc) (**5**) by insertion of carbon dioxide into the Ni–C bond of (^{tBu}PBP)NiMe (**1**) is presented. An unexpected CO_2 cleavage process involving the formation of new B–O and Ni–CO bonds leads to the generation of a butterfly-structured tetra-nickel cluster (^{tBu}PBOP)$_2$Ni$_4$(μ-CO)$_2$ (**6**). Mechanistic investigation of this reaction indicates a reductive scission of CO_2 by O-atom transfer to the boron atom via a cooperative nickel-boron mechanism. The CO_2 activation reaction produces a three-coordinate (^{tBu}P$_2$BO)Ni-acyl intermediate (**A**) that leads to a (^{tBu}P$_2$BO)–Ni^{I} complex (**B**) via a likely radical pathway. The Ni^{I} species is trapped by treatment with the radical trap (2,2,6,6-tetramethylpiperidin-1-yl)oxyl (TEMPO) to give (^{tBu}P$_2$BO)Ni^{II}(η^2-TEMPO) (**7**). Additionally, ^{13}C and ^{1}H NMR spectroscopy analysis using ^{13}C-enriched CO_2 provides information about the species involved in the CO_2 activation process.

Introduction

The design of ligands that can modulate the electronic and steric properties of transition metal complexes is a powerful strategy that has allowed the discovery of new modes of reactivity potentially relevant in catalysis. In particular, the development of ligands that cooperate with the metal center for the activation of kinetically inert molecules is an area of growing interest that is attracting the attention of many researchers.[1] One important contribution to this field was the synthesis of a new family of pincer ligands based on boron and phosphorus by Nozaki and Yamashita in 2009,[2] the bis-phosphino boryl (PBP) pincer ligands represented in Figure 1.

Rapid progress on the coordination chemistry with transition metals of PBP ligands has provided information on the key role of the boryl group for the reactivity of these complexes.[3] In 2013, Peters and co-workers reported the cooperative activation of H_2 by PBP-cobalt complexes[4] and, simultaneously with us, by nickel compounds.[5,6] We described a mechanism mediated by (^{t}Bu-PBP)NiMe (**1**, Scheme 1) that involves cooperation between the nickel center and both the boryl and methyl groups in the H–H bond breaking event through a five center transition state (Scheme 1, via TS1). The heterolytic cleavage of H_2 gives the nickel hydride species **2** through the intermediacy of a Ni^0 σ-BH complex for which the boryl moiety acts as a Lewis acid accepting a hydride while the methyl group acts as a Lewis base receiving a proton.[6]

The role of boron as a Lewis acid in transition metal-boron cooperative mechanisms, either mediated by a metal-borane or a metal-boryl complex, has been established by

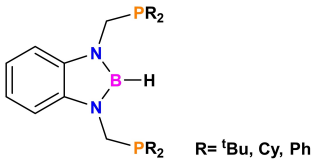

Figure 1. PBP ligands reported by Yamashita and Nozaki.[2]

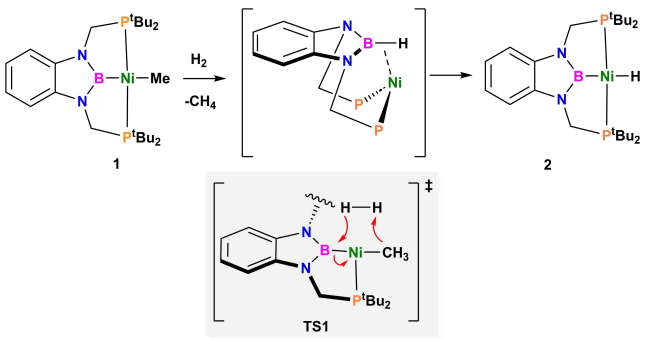

Scheme 1. H_2 activation by (^{t}Bu-PBP)NiMe (**1**).

[*] Dr. L. Álvarez-Rodríguez, Dr. P. Ríos, Dr. C. J. Laglera-Gándara, A. Jurado, Dr. F. J. Fernández-de-Córdova, Dr. A. Rodríguez
Instituto de Investigaciones Químicas-Departamento de Química Inorgánica, Universidad de Sevilla-Consejo Superior de Investigaciones Científicas, Centro de Innovación en Química Avanzada (ORFEO-CINQA)
C/Américo Vespucio 49, 41092 Sevilla (Spain)
E-mail: marodriguez@iiq.csic.es
Prof. T. B. Gunnoe
Department of Chemistry, University of Virginia
Charlottesville, VA 22904 (USA)
E-mail: tbg7h@virginia.edu

different groups in the last decade.[7] Owen and co-workers demonstrated the ability of a transition metal-*borane* complex to activate H_2.[8] One year later, Peters and co-workers reported the heterolytic cleavage of dihydrogen using a nickel complex stabilized by a bis(phosphino)*borane* ligand for which the boron center and the metal behave as hydride and proton acceptors, respectively.[9] Extension of this reactivity to other metals (e.g., Fe, Co, Pt) and other substrates with different E–H bonds (E=Si, C, N, O, S) corroborated the general behavior of boron as a cooperative electrophile.[10] However, we have recently found that the electrophilic role of the boron center can be controlled by the ligand *trans* to it, demonstrating its ambiphilic nature. Replacement of the methyl group in **1** by a catecholboryl moiety has an impact on the reactivity of the diaminoboryl group on the ligand. The new species (^{t}Bu-PBP)Ni(Bcat) (**3**, Scheme 2) reacts with H_2 through a mechanism similar to that observed for **1**, but now the diaminoboryl group behaves as a Lewis basic site and, after the heterolytic cleavage of the H–H bond, a B–H bond is formed by proton transfer to this boron atom (via TS2 in Scheme 2).[11]

This interesting reactivity based on metal-boron cooperative pathways served as a motivation to test the ability of ^{t}Bu-PBP-nickel methyl complex (**1**) for the activation of inert molecules such as carbon dioxide.[12a] Recently, Hazari and co-workers have reported an in-depth analysis of the insertion of carbon dioxide for a family of R-PBPMCH$_3$ species (R = ^{t}Bu, Cy; M=Ni, Pd) to form the corresponding acetate

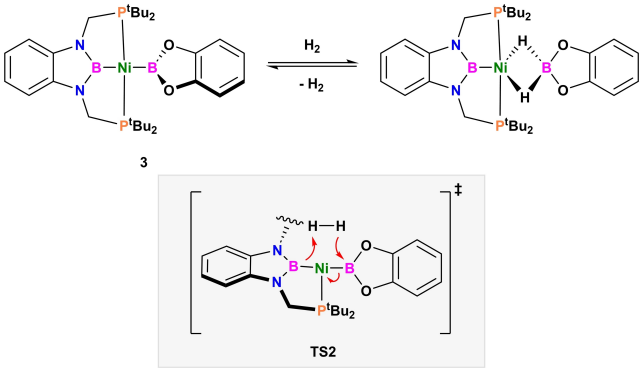

Scheme 2. Reversible H_2 activation mediated by **3**.

complexes, which demonstrates the impact of the bulkiness of the ligand and the solvent on the reaction rate.[12b] Previously, our group found that the ^{t}Bu-PBP-nickel hydride complex (^{t}Bu-PBP)NiH (**2**) is an active catalyst for selective hydrosilation of carbon dioxide to form aldehydes when used in combination with $B(C_6F_5)_3$.[12c,d] The formate species (^{t}Bu-PBP)Ni(O_2CH) (**4**) is instantly observed after CO_2 insertion into the Ni–H bond, but, in the absence of borane, the formation of different unidentified species is observed with no observation of catalysis.[12c–e] Intrigued by this result, we decided to investigate the reactivity of carbon dioxide in detail using complex **1**. Herein, we present our analysis of the cooperative mechanism of the activation of CO_2 promoted by the nickel-boron bond of **1** that ends with cleavage of one of the C–O bonds and release of carbon monoxide.

Results and Discussion

As mentioned above, we have previously studied the insertion of carbon dioxide into the nickel-hydride bond of **2**. As expected, the strong *trans* influence of the boryl ligand favors the instantaneous formation of nickel formate complex **4**.[12c] This species is thermally unstable, and a complex reaction mixture was observed by ^{31}P NMR spectroscopy when a solution of **4** was heated at 70 °C. To better understand the factors underlying this reactivity, we extended this study to the insertion of CO_2 into the nickel-carbon bond of **1**. Compared to insertions of CO_2 into Ni–H bonds, examples of analogous reactions with Ni–C bonds are less frequently reported and generally require more drastic reaction conditions (i.e., higher temperature and/or longer reaction times).[13,14] Here, the high *trans* influence of the boryl fragment increases the nucleophilicity of the methyl group and likely facilitates the CO_2 insertion process. Accordingly, when CO_2 (3 bar) was added to a solution of **1** in C_6D_6, the ^{31}P{^{1}H} NMR spectrum showed, after 16 hours at 40 °C, 90 % conversion of **1** to a new species identified as the acetate complex **5** on the basis of ^{31}P, ^{11}B, ^{1}H and ^{13}C NMR spectroscopic data (Scheme 3). Complex **5** exhibits a singlet at 84.9 ppm in the ^{31}P{^{1}H} NMR spectrum and a new signal in the ^{11}B{^{1}H} spectrum at 36 ppm, which is characteristic of a nickel-boryl bond.[15] The ^{1}H NMR spectrum shows a singlet at 2.25 ppm, which correlates with a signal in the ^{13}C{^{1}H}

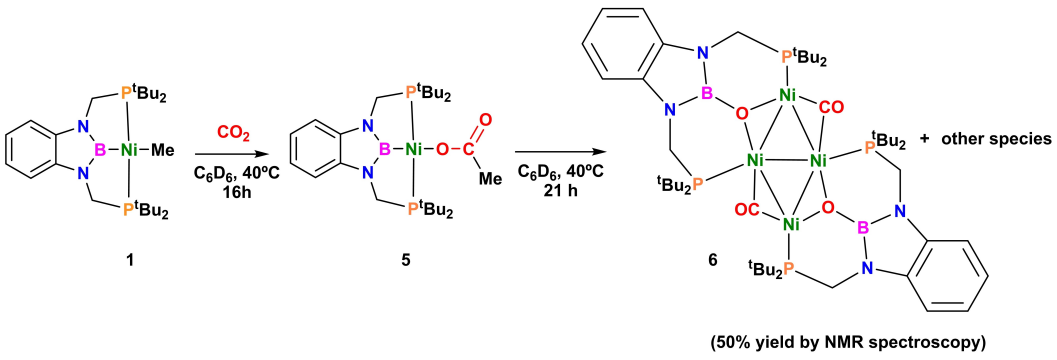

Scheme 3. Synthesis of (^{tBu}PBOP)$_2$Ni$_4$(μ-CO)$_2$ (**6**).

NMR spectrum (^{1}H,^{13}C-HMQC) at 25.8 ppm. The peak at 2.25 ppm can be assigned to the methyl protons of the acetate group. Additionally, the carbonyl group resonates at 174.8 ppm in the $^{13}C\{^{1}H\}$ NMR spectrum. Crystals suitable for X-ray diffraction analysis were obtained by cooling a C_6D_6/pentane solution of **5**.[16] The molecular structure of **5** is shown in Figure 2.

The nickel atom of **5** adopts a distorted square planar geometry with a κ^1-O-coordinated acetate group almost perpendicular to the main plane of the molecule. The Ni–B bond length (1.902(2) Å) of **5** is similar to those observed for ^{tBu}PBP-nickel complexes **1**–**4**.[5,6,11] The Ni–O1 bond length (1.951(2) Å) falls in the range observed for related nickel acetate complexes previously reported by Zargarian and Wendt,[13,14] and it is virtually identical to that reported for the formate complex **4**.[5] Interestingly, Hazari and co-workers[12b] reported the observation of unidentified decomposition products (20 %) along with nickel methyl complex **1** (30 %) when **1** was treated with CO_2 (1 atm) at room temperature for 10 days. Under these reaction conditions, isolation of the acetate complex was not possible, and the formation of **5** is proposed based on its $^{31}P\{^{1}H\}$ NMR spectrum by analogy with that observed for the derivative with cyclohexyl groups on phosphorus.[17a–c]

Careful control of the temperature and time of the reaction of **1** with CO_2 is required to avoid further reactivity of complex **5**. We have observed that prolonged heating of solutions of **5** gives rise to new species whose $^{31}P\{^{1}H\}$ and ^{1}H NMR spectra are almost identical to those obtained previously by heating solutions of formate complex **4**. At this point, we were curious about the nature of these new species and the chemistry behind this reactivity. Monitoring the reaction of **1** with CO_2 (3 bar) at 40 °C over a period of 21 hours by $^{31}P\{^{1}H\}$ NMR spectroscopy shows the initial formation of **5** (δ_P 84.9 ppm) and its complete transformation into a new species. In the $^{31}P\{^{1}H\}$ spectrum, the disappearance of the signal at 84.9 ppm was accompanied by the appearance of three signals at 51.0, 36.5 and 10.7 ppm in an approximate 1:1:2 ratio with a minor peak at 14 ppm (see Figure S15). From this reaction mixture, we were able to isolate compound **6** in pure form by crystallization (Scheme 3).[17c] Complex **6** features a broad ^{11}B resonance at considerably higher field (25 ppm) than that observed for complex **5** (36 ppm) and two signals at 51.0 and 36.5 ppm in the $^{31}P\{^{1}H\}$ NMR spectrum that correspond to two inequivalent phosphorous atoms. The ^{1}H NMR spectrum of **6** exhibits four different resonances for both the CH_2 and the CH_3 protons due to the reduced symmetry of the molecule. These signals are identical to those observed after thermal decomposition of the (^{t}Bu-PBP)Ni(O_2CH) (**4**) formate species. Deep red crystals suitable for X-ray diffraction analysis were obtained by cooling pentane solutions of **6** at −23 °C (Figure 3).

The solid-state structure of **6** reveals an unexpected nickel cluster made up of four nickel atoms in a butterfly structure and bridged together by two μ-CO groups and two (κ^3-*P,O,P*-μ_2-*O*)^{tBu}PBOP ligands. Each PBOP ligand spans between two nickel atoms of each of the dinickel subunits with the O atom connected to both nickel centers to form two fused six membered rings [(NiPCNB)$_2$(μ_2-O)]. Complex **6** has a mixed-valent $(Ni_4)^{+2}$ core, considering the overall charge of the PBOP ligands as −2 whereas CO ligands are neutral, which is consistent with two nickel centers with a formal oxidation state +1 and the other two being Ni^0. Ni–Ni bond lengths values, from 2.3727(7) to 2.4912(6) Å, correlate well with those previously reported for Ni^0-Ni^I bonds.[18] The Ni2-Ni4 bond length (2.6456(6) Å) is in the upper range for typical Ni^I-Ni^I bond lengths (from 2.291 to 2.605 Å),[19] but the diamagnetic character of this molecule is indicative of a clear contact between both metal atoms. Indeed, DFT calculations on **6** indicate a singlet configuration as the ground state (see Supporting Information for more details).

Analysis of the spin density revealed that this is predominantly located on d orbitals of Ni2 and Ni4 with a spin population of 0.807 on each metal, which is in agreement with two Ni^I centers (Figure 4). However, the opposite sign of both spins (one α spin and one β spin) account for the antiferromagnetic coupling that is experimentally observed.

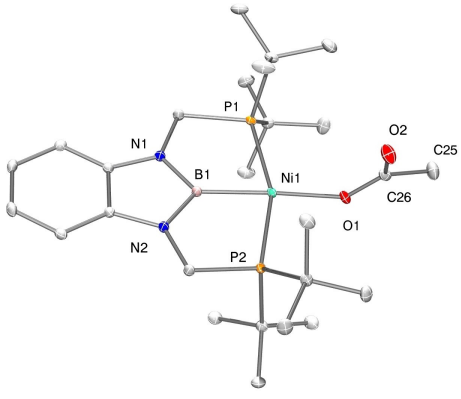

Figure 2. ORTEP of complex **5** at the 30% probability level. Hydrogen atoms are omitted for clarity. Selected bond lengths (Å) and angles (°): B(1)–Ni(1) = 1.902(2); Ni(1)–O(1) = 1.951(2); O(1)–C(26) = 1.274(4) ; C(26)–O(2) = 1.229(3); Ni(1)-O(1)-C(26) = 125.3(2); P(1)–Ni(1)–P(2) = 158.68(2); B(1)–Ni(1)–O(1) = 172.33(8).

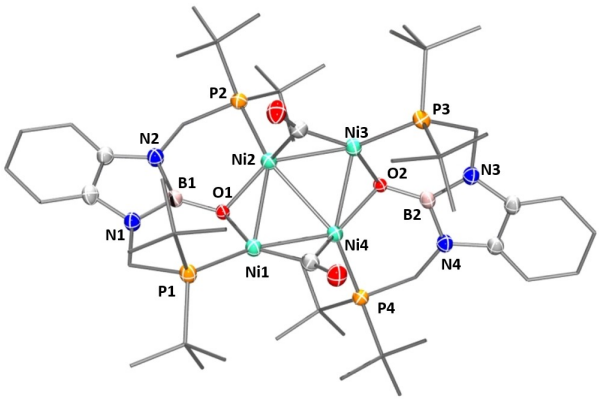

Figure 3. Molecular structure of complex **6** at the 30% probability level. Hydrogen atoms are omitted for clarity. Selected bond lengths (Å): Ni1–Ni2 = 2.4912(6); Ni2–Ni3 = 2.3727(7); Ni3–Ni4 = 2.4894(7); Ni4–Ni1 = 2.3876(6); Ni2–Ni4 = 2.6456(6).

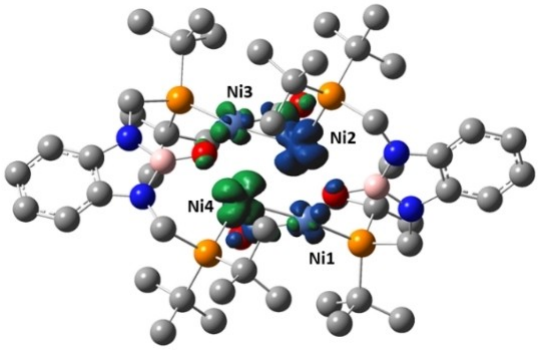

Figure 4. Spin density distribution of complex **6** (isovalue = 0.005) calculated at the UPBE0-D3/6–31 g(d,p) level of theory. Spin density values: Ni1 = 0.078; Ni2 = 0.807; Ni3 = -0.078; Ni4 = -0.807.

Thus, computational data support the oxidation state assignment described above (i.e., two Ni^{I} and two Ni^{0} centers).

The formation of the $(Ni_4)^{+2}$ core of **6** involves a redox process for which the Ni^{II} acetate complex is reduced to Ni^{I} and Ni^{0} species leading to the formation of **6** from **5**. We performed radical trapping experiments that provide evidence for the formation of a Ni^{I} intermediate after activation of carbon dioxide (see below). Moreover, the two newly formed B–O bonds are consistent with a process that implicates the abstraction of an oxygen atom from CO_2 by boron to form one equivalent of Ni-coordinated CO. These two facts caught our attention mainly because two interesting reactions might be involved: (i) activation of CO_2 mediated by a nickel methyl complex, and further reduction of CO_2 to CO by (ii) cleavage of one of the C=O bonds of CO_2 through a cooperative mechanism promoted by the nickel-boron bond.

In the chemical industry, CO is a common raw material widely used in many important processes including, for instance, the Monsanto acetic acid process, hydroformylation, the Water Gas Shift reaction and the Fischer–Tropsch reaction, to name a few. Currently, CO is predominantly made from methane via steam methane reforming. However, the utilization of CO_2 as innocuous and abundant source of carbon monoxide is of interest for the development of sustainable chemical processes. In this regard, the electrochemical reduction of CO_2 to CO using renewable sources is considered a very promising approach for the production of value added carbon-containing products.[20] Yet, the transformation of CO_2 into CO requires the cleavage of one of the C=O bonds of CO_2, which is a challenging reaction considering the high strength of its C=O bonds and its generally unreactive nature.[21] In nature, reversible transformation of CO_2 to CO is catalyzed by carbon monoxide dehydrogenase enzymes that possess an Fe–Ni active site to promote CO_2 activation and reduction. The mechanism of this reaction is not yet fully understood, but the formation of a Ni–C-(O)O–Fe intermediate was recently demonstrated by X-ray diffraction.[22]

Design of synthetic metallic systems capable of promoting the reduction of CO_2 to CO could help to understand this transformation in nature. Moreover, in a future for which green hydrogen is commercially viable, its utilization to transform CO_2 to CO could compete with current syngas processes to generate CO. Early examples of synthetic catalysts for CO_2 fixation were based on precious metals (Ru, Ir, Rh, Pd),[23] but, recently, growing interest in catalysts based on earth-abundant metals has resulted in the development of first row transition metal complexes that effectively reduce CO_2 to CO.[24–27] Bimetallic Fe–Ni systems that simulate the role of the Fe–Ni active site in CO dehydrogenase have been described.[27a,b] Likewise, metal-ligand cooperation strategies have emerged as an interesting approach for the design of systems that function as [Fe–Ni]-CODH models. Mechanistic investigations have revealed unique modes of CO_2 activation that could be integrated into new catalytic processes.[27] Our PBP–Ni complex **1** combines both a basic site at the methyl group and an electrophilic boron center at the central position of the ligand, which might provide new reactivity patterns based on *boryl-nickel-methyl cooperative* pathways for CO_2 activation.

With this idea in mind, to gain insight into the mechanism of the reaction of **1** with CO_2, we monitored the reaction of **1** with ^{13}C-enriched CO_2 by ^{1}H and ^{13}C NMR spectroscopy. The data extracted from this experiment related to the ^{13}C-enriched species formed during this reaction offer relevant information. Initially, the resonance corresponding to the methyl group of the acetate appears, in the ^{1}H NMR spectrum, as a doublet at 2.25 ppm ($^{2}J_{CH} = 6$ Hz), and the signal for the carbonyl group is clearly observed in the $^{13}C\{^{1}H\}$ NMR spectrum at 174.6 ppm. As the reaction progresses, the resonances of the acetate group disappear, and the formation of a new species in the ^{1}H NMR spectrum is observed at 1.54 ppm (d, $^{2}J_{CH} = 6$ Hz) that correlates (^{1}H,^{13}C-HMBC) with a peak in the $^{13}C\{^{1}H\}$ spectrum at 203.7 ppm. These chemical shift values match those of acetone.[28] In addition, a signal at 256.4 ppm is observed in the $^{13}C\{^{1}H\}$ NMR spectrum, which corresponds to ^{13}C enriched CO ligands present in **6**. No other ^{13}C-labelled species were observed (Figure S17). Release of CO is not detected, and when this solution was exposed to 2 bar of CO (12 h at 70 °C) no ^{13}CO/CO exchange was observed.

Although a mechanistic scenario involving Ni^{II} species cannot be completely discarded, the formation of acetone and the existence of a mixed valence Ni^{I}/Ni^{0} core in **6** raises the question about the possible involvement of Ni^{I} species in the formation of **6** through a radical mechanism. To confirm this hypothesis, we performed the reaction of **1** with CO_2 in the presence of the stable radical TEMPO {(2,2,6,6-tetramethylpiperidin-1-yl)oxyl}. Interestingly, after 12 h at 40 °C the only species detected was acetate complex **5**, and prolonged heating at higher temperatures (up to 80 °C) did not lead to the formation of **6**. We hypothesize that, in the presence of TEMPO, under these reaction conditions, an interaction between boron and TEMPO inhibits the process leading to the cleavage of the C–O bond.[29] Nevertheless, at 90 °C complex **5** evolves to a new species **7** (68 % spectroscopic yield) (Scheme 4). The $^{31}P\{^{1}H\}$ NMR spectrum of **7** consists of two signals at 56.3 and 11.1 ppm and the $^{11}B\{^{1}H\}$ spectrum exhibits a signal at 23 ppm, similar to that of **6**. Suitable crystals for an X-ray diffraction analysis were

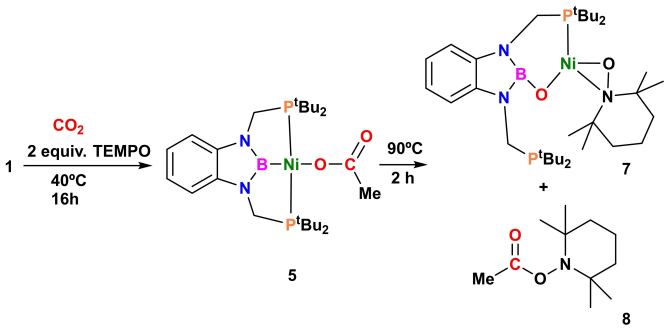

Scheme 4. Reaction of **1** with CO_2 in the presence of TEMPO.

obtained by cooling a toluene/pentane solution of **7** at −23 °C (Figure 5).

The solid-state structure of **7** shows a distorted square planar geometry at nickel with a η^2-*N,O*-coordinated TEMPO ligand and, as a consequence, one of the phosphine arms of the ligand has dissociated from the metal center. The structure of the PBP ligand is altered by the insertion of an O atom into the Ni–B bond to form a six-membered ring (NiPCNBO). The three membered Ni–O–N metallacycle is characterized by Ni–O, O–N, and Ni–N bond lengths of 1.834(1), 1.390(2), 1.926(2) Å and an acute O–Ni–N angle of 43.31(6)°. These values are consistent with an anionic η^2-TEMPO ligand coordinated to nickel that is generated by electron transfer from a Ni^I species to TEMPO, affording the Ni^{II}-TEMPO complex **7**.[30] Additionally, GC-MS analysis of the crude reaction mixture provided a signal at m/z = 199.15, which corresponds to the TEMPO-acyl adduct (**8**),[30c] confirming that the reaction likely follows a pathway that involves an acyl radical species (Scheme 4; Figures S18–20).

We propose that the formation of both **6** and **7** might occur by homolytic dissociation of the nickel-carbon bond of a nickel acyl complex (**A** in Scheme 5), formed by boron-assisted C–O bond activation of the acetate moiety of **5**. In this process, Ni^I fragments (**B** in Scheme 5, see below), which constitute the building blocks of the structure of complex **6** (and **7**), are generated.

Furthermore, the concomitant formation of acetone in the reaction might be explained by the combination of acyl radicals with methyl radicals (generated from the decarbonylation of the former) as shown on the equations (1) and (2).[31]

$$CH_3\dot{C}O \longrightarrow {}^{\bullet}CH_3 + CO \quad (1)$$

$$CH_3\dot{C}O + {}^{\bullet}CH_3 \longrightarrow (CH_3)_2CO \quad (2)$$

Interestingly, Holland, Cundari and co-workers have observed similar reactivity when they attempted to synthesize three-coordinate Ni^{II} methyl species. Instead of obtaining Ni^{II} derivatives, they observed the oxidation of methyl by nickel to yield a Ni^I complex along with ethane and methane by recombination of the resulting methyl radical.[32] To explore whether a similar process takes place in the formation of **6**, we investigated the possibility of generating the three-coordinate nickel-acyl species **A** (Scheme 5) by insertion of CO into (PBO)nickel-methyl species **C** (Scheme 6). We thought that treatment of **1** with trimethylamine *N*-oxide would lead to **C**, but, instead, the formation of new species $(PBO)_2Ni$ (**12**) (85 % spectroscopic yield) along with the release of ethane was observed.

The molecular structure of **12**, determined by single-crystal X-ray diffraction analysis, confirms the insertion of an O atom into the Ni–B bond to generate a Ni^{II} center

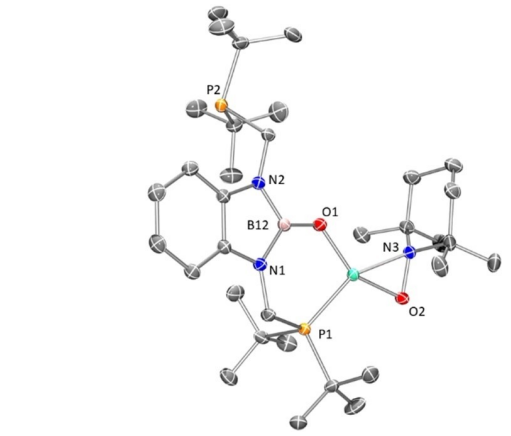

Figure 5. Molecular structure of complex **7** at the 30% probability level. Hydrogen atoms are omitted for clarity. Selected bond lengths (Å) and angles (°): Ni1–O1 = 1.846(1); Ni1–P1 = 2.1785(6); Ni1–O2 = 1.834(1); B12–O1 = 1.318(3); Ni1–N3 = 1.926(2); N3–O2 = 1.390(2); N3–Ni1–O2 = 43.31(6).

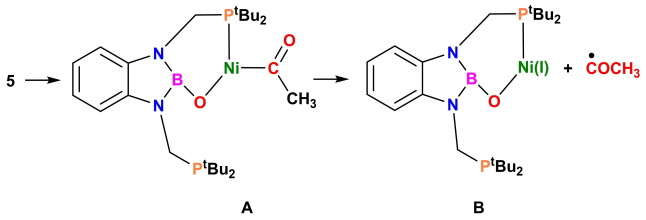

Scheme 5. Proposed initial reaction for the formation of **7** and **8** from complex **5**.

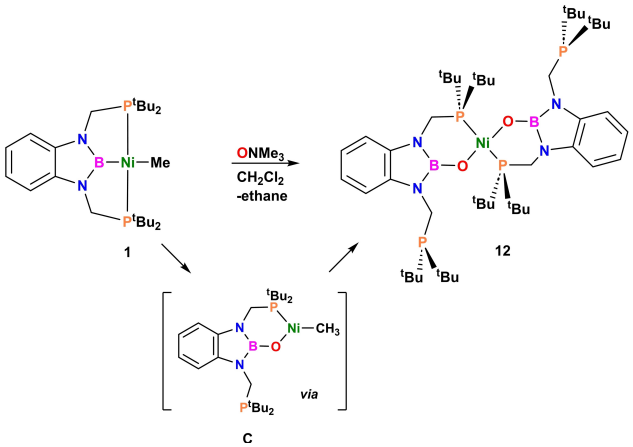

Scheme 6. Reaction of **1** with trimethylamine *N*-oxide.

surrounded by two PBO ligands in a distorted square-planar geometry (Figure S38).

The formation of **12** is likely due to the initial generation of an unstable (PBO)Ni-methyl species **C** that undergoes homolytic Ni–C bond cleavage leading to the formation of ethane and a (PBO)Ni^{I} species that disproportionates to give Ni^{II} complex **12** and metallic Ni(s). Monitoring this reaction by ^{31}P and ^{1}H NMR spectroscopy shows the initial formation of two intermediates, species **13a** and **13b**, that, over the course of 5 days, evolve to **12** with the generation of ethane. Both species show very similar $^{31}P\{^{1}H\}$ NMR spectra characterized by two signals at 14.3 and 41.4 ppm for **13a** and 9.3 and 50.3 ppm for **13b**. In the ^{1}H NMR spectrum, two doublets, one at −1.17 ppm for **13a** and the other one at −0.85 ppm for **13b**, that exhibit three-bond ^{1}H–^{31}P coupling of approximately 4 Hz, are consistent with the presence of methyl groups. From this reaction mixture we were able to crystalize intermediate $[NiCH_3]_2(\mu\text{-}\kappa^3\text{-POP})(\mu\text{-O})$ (**13a**). Single crystal X-ray diffraction analysis reveals a dinuclear structure consistent with two nickel atoms in a square-planar geometry connected by two PBOP ligands; one of them displays a $\mu\text{-}\kappa^3$-P,O,P-coordination while the other acts as a bridging oxo ligand with both phosphorous atoms not coordinated to nickel. The fourth coordination site at each nickel is occupied by a methyl group (Figure 6). Redissolution of these crystals in CD_2Cl_2 showed progressive transformation of **13a** into **13b**, both species coexisting, along with the appearance of **12** and formation of ethane. Since the ^{1}H DOSY NMR experiment is not consistent with an equilibrium between a monomeric and dimeric nickel species, it seems reasonable to propose that **13a** and **13b** are geometric isomers that interconvert by coordination/decoordination of the phosphine arms of both ligands.

As mentioned above, we hypothesize that similar species, containing an acyl group (**A** in Scheme 5) might be involved in the formation of **6**. Nevertheless, analogous species to **13** bearing an acyl group should also be considered. To probe this possibility, we performed the reaction of **13** with 1 bar of CO and observed the formation of **6** as the major product of the reaction, along with release of dimethyl ketone, after 12 h at room temperature in C_6D_6 solution (see SI, Figures S42–43).

Although the corresponding nickel acyl species was not detected, these results provide reasonable evidence for the involvement of species analogous to **13** in the growth process leading to the formation of **6**.

However, this reactivity does not explain the presence of two Ni^{0} atoms in **6** (Scheme 7). As mentioned before, the formation of **6** is accompanied by the generation of a new species (in a 1:1 ratio) whose chemical shift in the $^{31}P\{^{1}H\}$ NMR spectrum (δ 10.7 ppm; see above) is very close in chemical shift to that of the ^{tBu}PB(OH)P ligand (**10**) (δ 11.0 ppm) (independently synthetized by treatment of ^{tBu}-PBPOMe (**9**) with water; see SI, Figures S21–29).[33] Its ^{1}H and $^{13}C\{^{1}H\}$ NMR spectra are slightly different, which indicates that these species might not be identical but are likely similar in nature (See SI, Figures S31–33). Finally, High Resolution Mass Spectroscopy (HRMS) indicates that this species corresponds to the bis(boryl)ether ^{tBu}PBPOPBP^{tBu} (**11**) (See SI, Figure S34). Considering the stoichiometry of the reaction, it is likely that the formation of **11** is related to the generation of Ni^{0} through a decomposition pathway (pathway 1 in Scheme 7) in competition with the formation of Ni^{I} species (pathway 2 in Scheme 7). Yet, unfortunately, we are unable to provide experimental evidence to prove the mechanism by which Ni^{0} species are generated and, therefore, alternative pathways should not be excluded.

Each step of the overall process is depicted in Scheme 7: Initially, **5** is generated by *CO_2 insertion* into the Ni–C bond of **1**. Then, *CO cleavage* mediated by nickel-boron coopera-

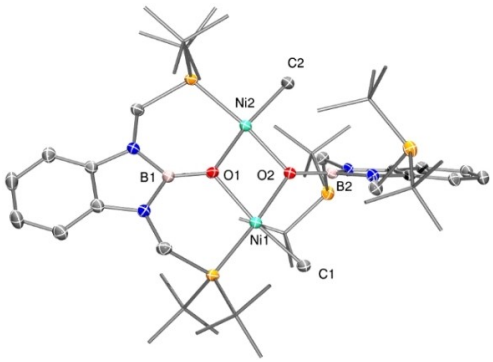

Figure 6. Molecular structure of complex **13a** at the 30% probability level. Hydrogen atoms are omitted for clarity. Selected bond lengths (Å): Ni1–O1 = 1.967(2); Ni1–O2 = 1.951(1); Ni2–O1 = 1.946(1); Ni2–O2 = 1.946(2); Ni1–C1 = 1.939(2); Ni2–C2 = 1.942(2).

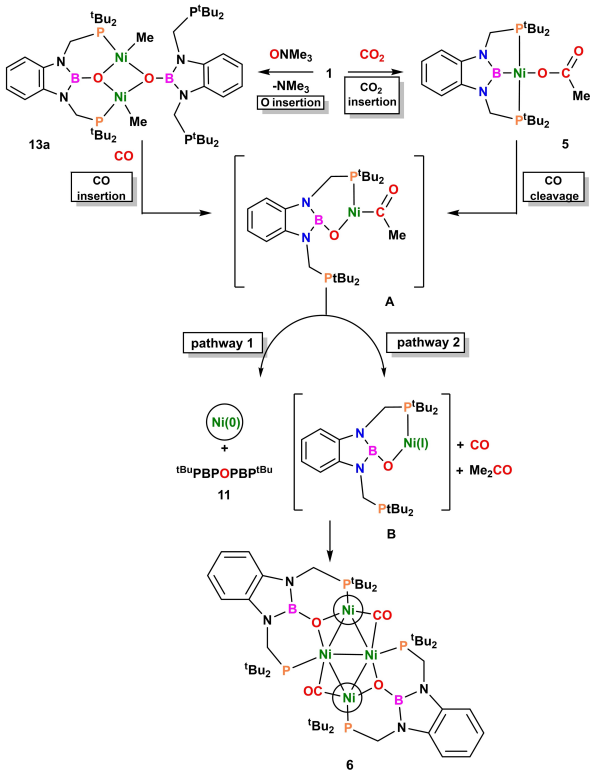

Scheme 7. Proposed pathway for the formation of **6**.

tivity generates nickel acyl intermediate **A** which evolves via two different pathways: i) release of bis(boryl)ether **11** and formation of Ni^0 (pathway 1) and ii) generation of Ni^I species (**B**) with concomitant formation of dimethylketone and carbon monoxide (pathway 2). These two processes lead to the formation of **6** in a complex reaction that combines Ni^0 and Ni^I species together with tBu-PBOP and CO ligands.

Conclusion

In summary, analysis of carbon dioxide insertion into the Ni–C bond of (^{tBu}PBP)NiMe (**1**) reveals unexpected reactivity promoted by the ability of the PBP ligand to cooperate with the metal center. Initially, the boryl group *trans* to the methyl moiety allows the formation of the expected nickel acetate complex **5** under mild reaction conditions. Then, one of the strong C=O bonds of carbon dioxide is cleaved to form a new B–O bond along with release of CO. In this step, the intermediacy of three-coordinate Ni^{II} acyl intermediates that evolve to Ni^I species through a radical mechanism has been proposed. The overall process involves the participation of $Ni^{II}/Ni^I/Ni^0$ species that ultimately results in the formation of a nickel cluster with butterfly structure bearing a $(Ni_4)^{+2}$ core. These results clearly demonstrate the potential of the *boryl-nickel* entity to activate strong bonds in inert molecules. Further studies on the activation and transformation of other small molecules may lead to unforeseen pathways of reactivity that can be valuable for future catalytic applications.

Acknowledgements

Financial support (FEDER contribution) from the MINECO (Projects PID2019/AEI/10.13039/50110001103 and RED2018-102387-T), Junta de Andalucía (Project PY20_00513) and the CSIC (AEPP-CTQ2016-76267-P) is gratefully acknowledged. TBG acknowledges the U.S. National Science Foundation under award CHE-2102433. C.J. L.-G. thanks for a Margarita Salas grant financed by the European Union-NextGenerationEU, Ministry of Universities and Recovery, Transformation and Resilience Plan, through a call from University of Oviedo (Grant MU-21-UP2021-030 53307942). P.R thanks Dr. Juan José Moreno for his assistance with spin density calculations and valuable discussion.

Conflict of Interest

The authors declare no conflict of interest.

Data Availability Statement

The data that support the findings of this study are available in the supplementary material of this article.

Keywords: Boryl Ligands · CO_2 Activation · Cooperativity · Nickel · Redox Chemistry

[1] a) J. I. van der Vlugt, *Eur. J. Inorg. Chem.* **2012**, 363; b) J. R. Khusnutdinova, D. Milstein, *Angew. Chem. Int. Ed.* **2015**, *54*, 12236; c) M. R. Elsby, R. T. Baker, *Chem. Soc. Rev.* **2020**, *49*, 8933.
[2] Y. Segawa, M. Yamashita, K. Nozaki, *J. Am. Chem. Soc.* **2009**, *131*, 9201.
[3] a) Y. Segawa, M. Yamashita, K. Nozaki, *Organometallics* **2009**, *28*, 6234; b) A. F. Hill, S. B. Lee, J. Park, R. Shang, A. C. Willis, *Organometallics* **2010**, *29*, 5661; c) M. Hasegawa, Y. Segawa, M. Yamashita, K. Nozaki, *Angew. Chem. Int. Ed.* **2012**, *51*, 6956; d) T. Miyada, M. Yamashita, *Organometallics* **2013**, *32*, 5281; e) H. Ogawa, M. Yamashita, *Dalton Trans.* **2013**, *42*, 625; f) H. Ogawa, M. Yamashita, *Chem. Lett.* **2014**, *43*, 664; g) A. F. Hill, C. M. A. McQueen, *Organometallics* **2014**, *33*, 1977; h) K. Tanoue, M. Yamashita, *Organometallics* **2015**, *34*, 4011; i) Y. Ding, Q.-Q. Ma, J. Kang, J. Zhang, S. Li, X. Chen, *Dalton Trans.* **2019**, *48*, 17633; j) F. Fang, M.-M. Xue, M. Ding, J. Zhang, S. Li, X. Chen, *Chem. Asian J.* **2021**, *16*, 2489; k) S. Hayashi, T. Murayama, S. Kusumoto, K. Nozaki, *Angew. Chem. Int. Ed.* **2022**, *61*, e202207760.
[4] T.-P. Lin, J. C. Peters, *J. Am. Chem. Soc.* **2013**, *135*, 15310.
[5] T.-P. Lin, J. C. Peters, *J. Am. Chem. Soc.* **2014**, *136*, 13672.
[6] N. Curado, C. Maya, J. López-Serrano, A. Rodríguez, *Chem. Commun.* **2014**, *50*, 15718.
[7] a) J. Takaya, *Chem. Sci.* **2021**, *12*, 1964; b) G. R. Owen, *Chem. Commun.* **2016**, *52*, 10712; c) M. Devillard, G. Bouhadir, D. Bourissou, *Angew. Chem. Int. Ed.* **2015**, *54*, 730.
[8] N. Tsoureas, Y.-Y. Kuo, M. F. Haddow, G. R. Owen, *Chem. Commun.* **2011**, *47*, 484.
[9] a) W. H. Harman, J. C. Peters, *J. Am. Chem. Soc.* **2012**, *134*, 5080; b) W. H. Harman, T.-P. Lin, J. C. Peters, *Angew. Chem. Int. Ed.* **2014**, *53*, 1081.
[10] a) S. N. MacMillan, W. H. Harman, J. C. Peters, *Chem. Sci.* **2014**, *5*, 590; b) D. L. M. Suess, J. C. Peters, *J. Am. Chem. Soc.* **2013**, *135*, 4938; c) D. L. M. Suess, J. C. Peters, *J. Am. Chem. Soc.* **2013**, *135*, 12580; d) J. S. Anderson, J. Rittle, J. C. Peters, *Nature* **2013**, *501*, 84; e) H. Fong, M.-E. Moret, Y. Lee, J. C. Peters, *Organometallics* **2013**, *32*, 3053; f) M. Nesbit, D. L. M. Suess, J. C. Peters, *Organometallics* **2015**, *34*, 4741; g) T. J. Del Castillo, N. B. Thompson, D. L. M. Suess, G. Ung, J. C. Peters, *Inorg. Chem.* **2015**, *54*, 9256; h) B. E. Cowie, D. J. H. Emslie, *Chem. Eur. J.* **2014**, *20*, 16899; i) B. R. Barnett, C. E. Moore, A. L. Rheingold, J. S. Figueroa, *J. Am. Chem. Soc.* **2014**, *136*, 10262; j) B. E. Cowie, D. J. H. Emslie, *Organometallics* **2015**, *34*, 4093.
[11] P. Ríos, J. Borge, F. Fernandez de Córdova, G. Sciortino, A. Lledós, A. Rodríguez, *Chem. Sci.* **2021**, *12*, 2540.
[12] a) R. Ayyappan, I. Abdalghani, R. C. Da Costa, G. R. Owen, *Dalton Trans.* **2022**, *51*, 11582; b) A. P. Deziel, M. R. Espinosa, L. Pavlovic, D. J. Charboneau, N. Hazari, K. H. Hopmann, B. Q. Mercado, *Chem. Sci.* **2022**, *13*, 2391; c) P. Ríos, N. Curado, J. López-Serrano, A. Rodríguez, *Chem. Commun.* **2016**, *52*, 2114; d) P. Ríos, A. Rodríguez, J. López-Serrano, *ACS Catal.* **2016**, *6*, 5715; e) The insertion of CO_2 into the nickel-hydride complex was simultaneously reported by Peters: See reference 5.
[13] a) T. J. Schmeier, N. Hazari, C. D. Incarvito, J. A. Raskatov, *Chem. Commun.* **2011**, *47*, 1824; b) A. H. Mousa, J. Bendix, O. F. Wendt, *Organometallics* **2018**, *37* 2581; c) A. H. Mousa, A. V. Polukeev, J. Hansson, O. F. Wendt, *Organometallics* **2020**, *39*, 1553.
[14] a) A. B. Salah, D. Zargarian, *Dalton Trans.* **2011**, *40*, 8977; b) K. J. Jonasson, O. F. Wendt, *Chem. Eur. J.* **2014**, *20*, 11894.

[15] S. Aldridge, D. L. Coombs, *Coord. Chem. Rev.* **2004**, *248*, 535.
[16] A substitutional disorder was found in the crystal. The acetate ligand is partially substituted by a bromine in a 91.5:8.5 ratio.
[17] a) We presume that at room temperature the full transformation of **1** into **5** is too slow to be observed in a reasonable period of time; b) The authors also mentioned that larger amounts of decomposition products were observed when the reaction with CO_2 was performed at higher temperature but their composition was not revealed. We have observed that very careful control of temperature and time is required to selectively obtain **5**; c) According to Hazari's observations, the transformation of nickel acetate **5** into **6** does not take place at room temperature after 10 days. Under these reaction conditions, some decomposition products are formed but their ^{31}P NMR chemical shift does not correspond to **6**.
[18] R. H. D. Lyngdoh, H. F. Schaefer, III, R. B. King, *Chem. Rev.* **2018**, *118*, 11626.
[19] Q. Dong, X. J. Yang, S. Gong, Q. Luo, Q. S. Li, J. H. Su, *Chem. Eur. J.* **2013**, *19*, 15240.
[20] J. Song, Z. Hao, K. Zhang, Z. Yan, J. Chen, *Angew. Chem. Int. Ed.* **2021**, *60*, 20627.
[21] a) D. deB. Darwent, *Bond Dissociation Energies in Simple Molecules*, National Bureau of Standards, NSRDS-NBS, 31 Washington, D. C., 1970; b) *CRC Handbook of Chemistry and Physics*, 73rd ed. (Ed.: D. R. Lide), CRC Press Inc., Boca Raton, **1992**.
[22] a) A. M. Appel, J. E. Bercaw, A. B. Bocarsly, H. Dobbek, D. L. DuBois, M. Dupuis, J. G. Ferry, E. Fujita, R. Hille, P. J. A. Kenis, C. A. Kerfeld, R. H. Morris, C. H. F. Peden, A. R. Portis, S. W. Ragsdale, T. B. Rauchfuss, J. N. H. Reek, L. C. Seefeldt, R. K. Thauer, G. L. Waldrop, *Chem. Rev.* **2013**, *113*, 6621; b) J.-H. Jeoung, H. Dobbek, *Science* **2007**, *318*, 1461.
[23] a) W. C. Kaska, S. Nemeh, A. Shlrazi, S. Potuznik, *Organometallics* **1988**, *7*, 13; b) M. A. McLoughlin, N. L. Keder, W. T. A. Harrison, R. J. Flesher, H. A. Mayer, W. C. Kaska, *Inorg. Chem.* **1999**, *38*, 3223; c) M. T. Whited, J. Zang, T. M. Donnell, V. H. Eng, P. O. Peterson, M. J. Trenerry, D. E. Janzen, B. L. H. Taylor, *Organometallics* **2019**, *38*, 4420.
[24] For representative examples with Fe, see: a) C. C. Lu, C. T. Saouma, M. W. Day, J. C. Peters, *J. Am. Chem. Soc.* **2007**, *129*, 4; b) A. R. Sadique, W. W. Brennessel, P. L. Holland, *Inorg. Chem.* **2008**, *47*, 784; c) C. T. Saouma, C. C. Lu, M. Day, J. C. Peters, *Chem. Sci.* **2013**, *4*, 4042; d) J. Leitl, M. Marquardt, P. Coburger, D. J. Scott, V. Streitferdt, R. M. Gschwind, C. Mgller, R. Wol, *Angew. Chem. Int. Ed.* **2019**, *58*, 15407; e) P. M. Jurd, H. L. Li, M. Bhadbhade, L. D. Field, *Organometallics* **2020**, *39*, 2011.
[25] For representative examples with Cu, see: a) D. S. Laitar, P. Müller, J. P. Sadighi, *J. Am. Chem. Soc.* **2005**, *127*, 17196; b) C. Kleeberg, M. S. Cheung, Z. Lin, T. B. Marder, *J. Am. Chem. Soc.* **2011**, *133*, 19060.
[26] For representative examples with Co, see: a) J. P. Krogman, B. M. Foxman, C. M. Thomas, *J. Am. Chem. Soc.* **2011**, *133*, 14582; b) L. Roy, M. H. Al-Afyouni, D. E. DeRosha, B. Mondal, I. M. DiMucci, K. M. Lancaster, J. Shearer, E. Bill, W. W. Brennessel, F. Neese, S. Ye, P. L. Holland, *Chem. Sci.* **2019**, *10*, 918; c) M. T. Whited, J. Zhang, A. M. Conley, S. Ma, E. Janzen, D. Kohen, *Angew. Chem. Int. Ed.* **2021**, *60*, 1615.
[27] For representative examples with Ni, see: a) C. Yoo, Y. Lee, *Chem. Sci.* **2017**, *8*, 600; b) J. R. Prat, C. A. Gaggioli, R. C. Cammarota, E. Bill, L. Gagliardi, C. C. Lu, *Inorg. Chem.* **2020**, *59*, 14251; For related reactivity see also: c) P. Zimmermann, D. Ar, M. Rößler, P. Holze, B. Cula, C. Herwig, C. Limberg, *Angew. Chem. Int. Ed.* **2021**, *60*, 2312; d) P. Zimmermann, S. Hoof, B. Braun-Cula, C. Herwig, C. A. Limberg, *Angew. Chem. Int. Ed.* **2018**, *57*, 7230; e) B. Horn, C. Limberg, C. Herwig, B. Braun, *Chem. Commun.* **2013**, *49*, 10923; f) Y.-E. Kim, J. Kim, Y. Lee, *Chem. Commun.* **2014**, *50*, 11458; g) C. H. Lee, D. S. Laitar, P. Mueller, J. P. Sadighi, *J. Am. Chem. Soc.* **2007**, *129*, 13802; h) R. J. Witzke, T. D. Tilley, *Chem. Commun.* **2019**, *55*, 6559; i) Y.-E. Kim, S. Oh, S. Kim, O. Kim, J. Kim, S. W. Han, Y. Lee, *J. Am. Chem. Soc.* **2015**, *137*, 4280; j) D. Sahoo, C. Yoo, Y. Lee, *J. Am. Chem. Soc.* **2018**, *140*, 2179; k) C. Yoo, Y.-E. Kim, Y. Lee, *Acc. Chem. Res.* **2018**, *51*, 1144; l) F. Schneck, J. Ahrens, M. Finger, A. C. Stückl, C. Würtele, D. Schwarzer, S. Schneider, *Nat. Commun.* **2018**, *9*, 1161; m) B. C. Fullmer, H. Fan, M. Pink, K. G. Caulton, *Inorg. Chem.* **2008**, *47*, 1865; n) D. Oren, Y. Diskin-Posner, L. Avram, M. Feller, D. Milstein, *Organometallics* **2018**, *37*, 2217; o) See also: J. S. Anderson, V. M. Iluc, G. L. Hillhouse, *Inorg. Chem.* **2010**, *49*, 10203.
[28] G. R. Fulmer, A. J. M. Miller, N. H. Sherden, H. E. Gottlieb, A. Nudelman, B. M. Stoltz, J. E. Bercaw, K. I. Goldberg, *Organometallics* **2010**, *29*, 2176.
[29] By carring out this reaction using an internal standard, it was confirmed by ^{31}P NMR that complex **5** remains intact and no other decomposition products are formed.
[30] a) D. J. Mindiola, R. Waterman, D. M. Jenkins, G. L. Hillhouse, *Inorg. Chim. Acta* **2003**, *345*, 299; b) D. Isrow, B. Captain, *Inorg. Chem.* **2011**, *50*, 5864; c) In the ^{1}H NMR spectrum signals corresponding to **8** were not observed. The concentration of this species is low probably because the trapping reaction of the acyl radical with TEMPO is not very effective. We did the reaction using $^{13}CO_2$ and we also observed, by ^{13}C NMR, formation of dimethylketone and 2,3-butanedione.
[31] See, for instance: a) I. Ryu, N. Sonoda, D. P. Curran, *Chem. Rev.* **1996**, *96*, 177; b) S. Bath, N. M. Laso, H. Lopez-Ruiz, B. Quiclet-Sire, S. Z. Zard, *Chem. Commun.* **2003**, 204; c) M. R. Heinrich, S. Z. Zard, *Org. Lett.* **2004**, *6*, 4969.
[32] a) P. L. Holland, T. R. Cundari, L. L. Pérez, N. A. Eckert, R. J. Lachicott, *J. Am. Chem. Soc.* **2002**, *124*, 14416; See also: b) M. H. Schofield, J. Halpern, *Inorg. Chim. Acta* **2003**, *345*, 353–358; c) T. J. Anderson, G. D. Jones, D. A. Vicic, *J. Am. Chem. Soc.* **2004**, *126*, 8100.
[33] ^{tBu}PBP(OMe) ligand was synthetized following a procedure previously described for the synthesis of related methoxyborane species, see: H. Kisu, T. Kosai, T. Iwamoto, M. Yamashita, *Chem. Lett.* **2021**, *50*, 293. The ^{1}H and ^{31}P NMR spectra of this compound are also similar to that observed for the by-product generated in the reaction of formation of **6** but not identical (See SI).
[34] Deposition numbers 2190215 (for **5**), 2190214 (for **6**), 2190213 (for **7**), 2253831 (for **12**) and 2253830 (for 1**3a**) contain the supplementary crystallographic data for this paper. These data are provided free of charge by the joint Cambridge Crystallographic Data Centre and Fachinformationszentrum Karlsruhe Access Structures service.

Manuscript received: May 8, 2023
Accepted manuscript online: July 3, 2023
Version of record online: July 17, 2023